NONLINEAR EFFECTS IN FIELD AMPLIFIED SAMPLE STACKING

Rajiv Bharadwaj[1], and Juan G. Santiago[2]
[1]Chemical Engineering Department, Stanford University, Stanford, CA 94305,
[2]Mechanical Engineering Department, Stanford University, Stanford, CA 94305

ABSTRACT

In field amplified sample stacking (FASS), the sample solution is typically prepared in low conductivity buffer or DI water, so that sample ion concentration can be on the order of the buffer ion concentration. Under these conditions, sample ions can strongly affect conductivity gradients and this leads to nonlinear dispersive effects due to electromigration. We have developed a model to investigate nonlinear electromigration dynamics for an electrolyte consisting of three fully ionized species. The model predicts two distinct regimes of concentration enhancement. For the single electrolyte-electrolyte interface system, the first regime is characterized by a rarefaction wave for the sample ion distribution with a final concentration enhancement which is greater than γ, the ratio of the conductivity of the background electrolyte and the sample solution. In the second regime, the sample ion concentration wave develops sharp gradients, steepening toward an ion concentration shock wave, and maximum concentration enhancement is less than γ. We have used scalar epi-fluorescence imaging to validate the model. A staggered-T glass microchip configuration was used for single buffer-buffer interface FASS experiments, under suppressed electroosmotic flow conditions. There is good quantitative agreement between the predicted and measured maximum concentration enhancement. The model can be used to optimize FASS under sample overloading conditions.

INTRODUCTION

Field amplified sample stacking (FASS) is a versatile sample preconcentration technique easily integrated with electrophoretic separations for both capillary[1-3] and microchip-based[4-6] systems. In FASS, an axial gradient in ionic conductivity (and therefore electric field) is achieved by preparing the sample in an electrolyte solution of lower concentration than the background electrolyte (BGE). Upon application of an axial potential gradient, the sample region acts as a high electrical resistance zone in series with the rest of the channel and a locally high electric field is generated within the sample zone. Under the influence of electric field, sample ions migrate from the high to low drift velocity region. This leads to a local accumulation or "stacking" of sample ions near the interface between the regions of high and low conductivity. This stacking increases sample concentration and results in an increased signal. More than 1000-fold signal increase is possible with this method.[4, 7]

Most descriptions of FASS process neglect the contribution of sample ions to the conductivity of sample plug. Although this assumption is valid for small sample-to-background electrolyte (BGE) concentration ratio, it leads to the well known result that the maximum concentration increase in FASS is proportional to γ, the ratio of conductivity of high concentration BGE and the sample.[1, 8] Since FASS relies on high conductivity ratios, the sample solution is typically prepared in low conductivity buffer or even deionized (DI) water.[1, 2] In such systems, sample ions can have a strong effect on local conductivity. For example, Chien and Burgi[2], and Chien[9] point out that for sample concentrations greater than 10 μM, conductivity gradients and pH fields can change during FASS injection and lead to complex behavior.

In this paper we analyze the effect of sample concentration on FASS efficiency. We have developed an unsteady electromigration model to investigate FASS dynamics in the limit of large electromigration-to-diffusive flux ratio. We have measured unsteady temporal and spatial sample ion concentration fields using full-field, quantitative epifluorescence microscopy to validate the model and suggest guidelines for optimized FASS systems.

THEORY

We consider one-dimensional electromigration of three, fully ionized ions: A (Counter-ion), B (co-ion) and C (sample ion). A constant current density, j_o, is applied in the axial direction and the electrolyte system is assumed to be electrically neutral. The electrophoretic mobility, ν, of various ions is assumed constant. We focus on FASS across single electrolyte-electrolyte interfaces as depicted in Figure 1. The system is assumed to have zero electroosmotic flow and we consider the limit of large electromigration-to-diffusive flux ratio and therefore neglect diffusion. In real systems, diffusion and convective contribute to dispersion and slow the FASS process.[8, 10]

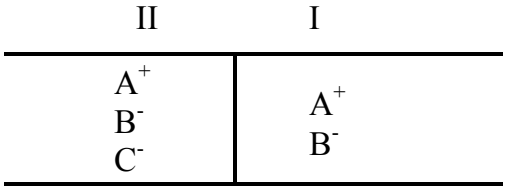

Figure 1: FASS system with a single sample/BGE interface. Roman numerals I and II denote high conductivity BGE and low conductivity sample regions, respectively.

Under these assumptions the governing equations are in dimensionless form:

$$E'(x,t) = \frac{1}{\sigma'(x,t)} \tag{1}$$

$$\frac{\partial C_A'}{\partial t'} = -z_A \frac{\partial}{\partial x}\left(\frac{C_A'}{\sigma'}\right) \tag{2}$$

$$\frac{\partial C_C'}{\partial t'} = -z_C \nu_C \frac{\partial}{\partial x}\left(\frac{C_C'}{\sigma'}\right) \tag{3}$$

Equation (1) is the condition of current conservation, and Equations (2) and (3) are the species conservation equation. The concentration of the third ion is determined by the electroneutrality condition:

$$C_B' = -\frac{\left(z_C C_C' + z_A C_A'\right)}{z_B} \tag{4}$$

The dimensionless variables are the following:

$$x' = \frac{x}{s}; v' = \frac{v}{v_A}; C' = \frac{C}{C_{Ao}}; \sigma' = \frac{\sigma}{F^2 v_A C_{Ao}}; t' = \frac{tj_o}{FsC_{Ao}} \tag{5}$$

where $\sigma(x,t) = F^2 \sum z_i^2 v_i C_i$ is the electrical conductivity distribution, s is the characteristic length scale of the initial concentration gradients, and C_{Ao}, is the initial counter-ion concentration in the sample region.

The boundary and initial conditions for the concentration fields are for the single electrolyte-electrolyte interface are

$$\begin{aligned} &C'_A(x' = -L', t') = \alpha; \quad C'_A(x = L', t') = 1; \quad \alpha > 1 \\ &C'_C(x' = -L', t') = 0; \quad C'_C(x = L', t') = \varepsilon. \end{aligned} \tag{6}$$

For a channel length, L, much larger than the characteristic interface length, s, we assume the following initial conditions ion distributions:

$$\begin{aligned} &C'_A(x', t' = 0) = 0.5((1+\alpha) + (1-\alpha) erf(x')) \\ &C'_C(x', t' = 0) = 0.5\varepsilon(1 + erf(x')) \end{aligned} \tag{7}$$

Here, $\varepsilon = C_{Co}/C_{Ao}$, is the ratio of the initial sample concentration and counter-ion concentration in the sample region and h' is the dimensionless sample plug length. We will drop the primes in the rest of the paper for clarity of presentation. We have used finite volume methods to solve the nonlinear hyperbolic equation governing sample ion distribution.

THEORETICAL RESULTS

The electromigration model developed sheds light on various important regimes of FASS dynamics. Figure 2a (i-iii) shows the spatial and temporal development of sample ion concentration field, C_C, the BGE ion concentrations, C_A and C_B, and electric field distribution for $\varepsilon << 1$. This situation, frequent in practice, is where a sample ion concentration, C_C, is much smaller than the BGE ion concentrations. In this limit, sample ions have a negligible effect on the conductivity field and the electrolyte system behaves as a binary electrolyte composed of A and B ions. The binary electrolyte in this simple case governs the conductivity distribution and hence the electric field. Sample ions act as a passive scalar whose electromigration is determined by the electric field distribution established by underlying BGE ions.

In figures 2b and 2c we study two cases where the sample ion concentration in the initial sample region is comparable to that of BGE ions, so that ε is order unity. As discussed earlier, this condition arises when the sample is prepared in very low conductivity buffer or DI water, and is also frequent in practice. Figures 2b(i-iii) show results for the case where the sample-ion-to-co-ion ratio of the product of electrophoretic mobility and valence number is less than unity, $\beta < 1$. Figure 2a(i) shows that the maximum concentration enhancement in this regime is lower than γ. Since $\beta < 1$, the sample ion wave velocity increases with sample concentration. This in turn implies a steepening of the concentration profile as the sample stacks, resulting in sharp gradients, and tending toward a concentration shock wave. Figure 2b(ii) shows the concentration

distribution of BGE ions, C_A and C_B. In this case, the BGE co-ion (C_B) and counter-ion (C_A) do not follow binary electrolyte dynamics and instead show complex migration behavior. The electric field shows a "two step" profile with two inflection points.

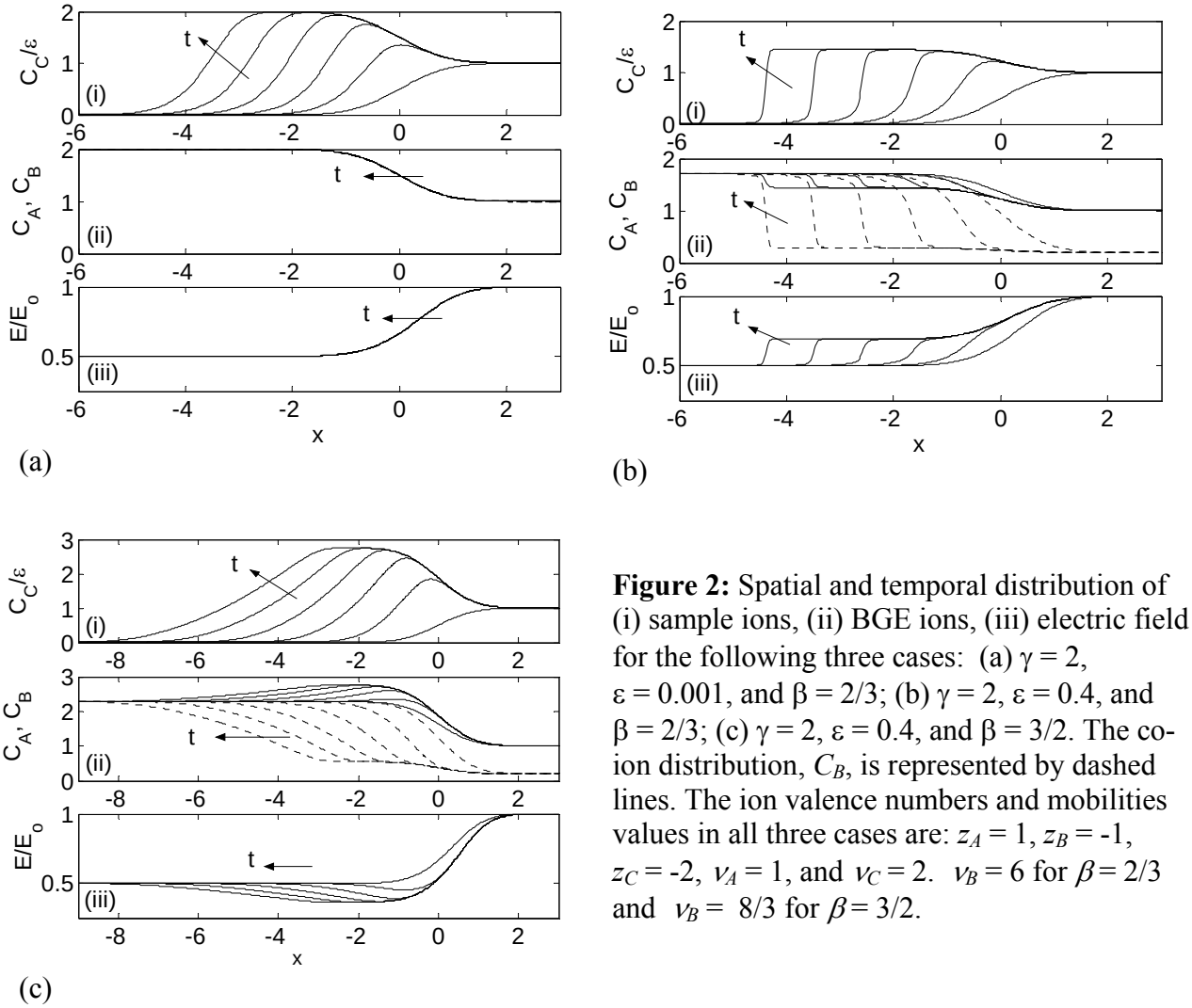

Figure 2: Spatial and temporal distribution of (i) sample ions, (ii) BGE ions, (iii) electric field for the following three cases: (a) $\gamma = 2$, $\varepsilon = 0.001$, and $\beta = 2/3$; (b) $\gamma = 2$, $\varepsilon = 0.4$, and $\beta = 2/3$; (c) $\gamma = 2$, $\varepsilon = 0.4$, and $\beta = 3/2$. The co-ion distribution, C_B, is represented by dashed lines. The ion valence numbers and mobilities values in all three cases are: $z_A = 1$, $z_B = -1$, $z_C = -2$, $\nu_A = 1$, and $\nu_C = 2$. $\nu_B = 6$ for $\beta = 2/3$ and $\nu_B = 8/3$ for $\beta = 3/2$.

Figure 2c describes the case of $\beta > 1$. For this case, concentration shocks do not form as sample ion wave velocity decreases with increasing sample concentration, and so concentration shocks cannot form. Further, the left edge of the concentration profiles becomes progressively "diffuse," despite the absence of diffusion (or any type of dispersion) in the model. Interestingly, the maximum concentration enhancement is higher than γ in this case.

EXPERIMENTAL RESULTS AND MODEL VALIDATION

An inverted epifluorescence microscope (Olympus IX70) equipped with a 10X objective (Olympus, NA = 0.4) and a 0.5X demagnifying lens was used for imaging the concentration fields of bodipy dye solutions. Images were captured using a cooled CCD camera (Cool-SNAP fx, Roper Scientific, Inc., Trenton, NJ) having a 1300 × 1030 array of square pixels, with 12-bit intensity resolution. A low fluorescence Borofloat glass microchip (Micralyne, Alberta, Canada)

with staggered-T channel geometry was used for all experiments. The microchannel width is 50 μm and the centerline depth of the channels is 20 μm.

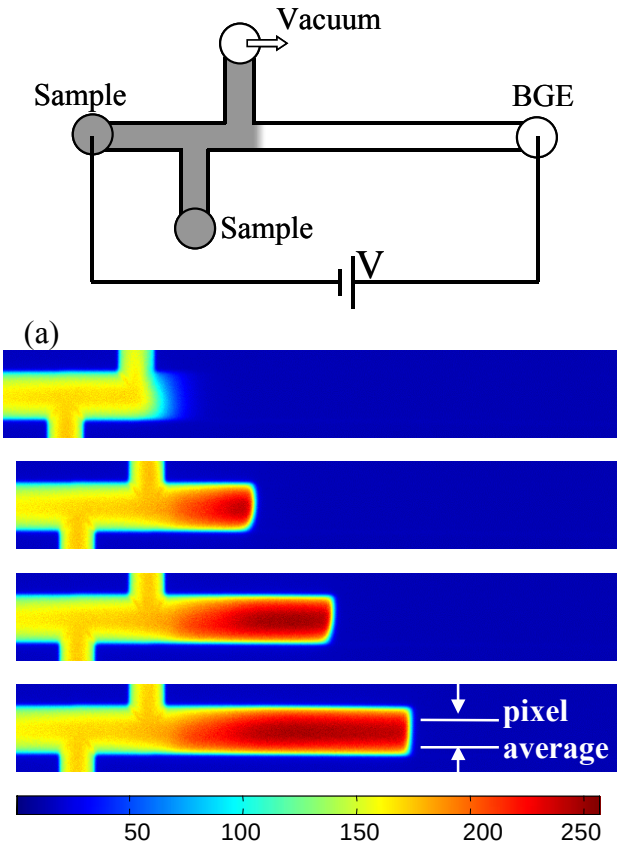

Figure 3: (a) Schematic of microchip system used for the experiments. A vacuum is applied to generate the initial conductivity gradient. Once the gradient is established, an electric field is applied from right-to-left to initiate stacking of negatively charged sample ions. (b) CCD Images showing development of sample ion concentration distribution. In this case $\gamma = 5$, $\beta = 0.25$, and $\varepsilon = 1$. At these conditions, the sample ion distribution tends toward a shock wave in concentration at the leading edge of the sample region. The time between each frame was 132 ms, and the applied nominal electric field was 176 V/cm.

To validate the model we have considered the $\beta < 1$ regime as a representative case of electromigration dispersion dynamics. This regime can be realized experimentally by using chloride ions as the co-ions, C_B. Chloride ions have a high electrophoretic mobility of 7.9e-8 m^2V/s [11]. The sample ion was negatively charged bodipy dye ($z_C = -1$, $\nu_C = 2e\text{-}8$ m^2V/s) [12]. The BGE was prepared by adding NaCl salt to deionized ultra-filtered (DIUF) water (Fisher Scientific, Baltimore, MD). An equal ratio of bodipy dye and sodium hydroxide was added to DIUF water to prepare the sample solution. The dye concentration was 198 μM in all cases. Experiments were performed for three conductivity ratios: $\gamma = 5$, 8.5, and 10. The microchip was flushed with acidified poly (ethylene oxide) solution to suppress electroosmotic flow (EOF) using the method described by Preisler and Yeung.[13] Electrical conductivity was measured using a conductivity meter (Pinnacle 542, Corning Inc., New York).

The interface between high and low conductivity electrolyte solutions was generated by applying a vacuum at the north reservoir of the microchip as shown in Figure 3a. Once the interface was established, the vacuum was released and an axial electric field was applied in the right-to-left direction. This initiates stacking of sample ions at the interface between the electrolyte streams. Figure 3b shows images of the stacking process at selected times. The instantaneous images show an increase in fluorescence intensity near the interface due to local accumulation of sample ions.

Also, the sample ion concentration gradients gradually become sharp and tends toward a sharp shock wave in concentration as predicted by the model for this $\beta < 1$ regime.

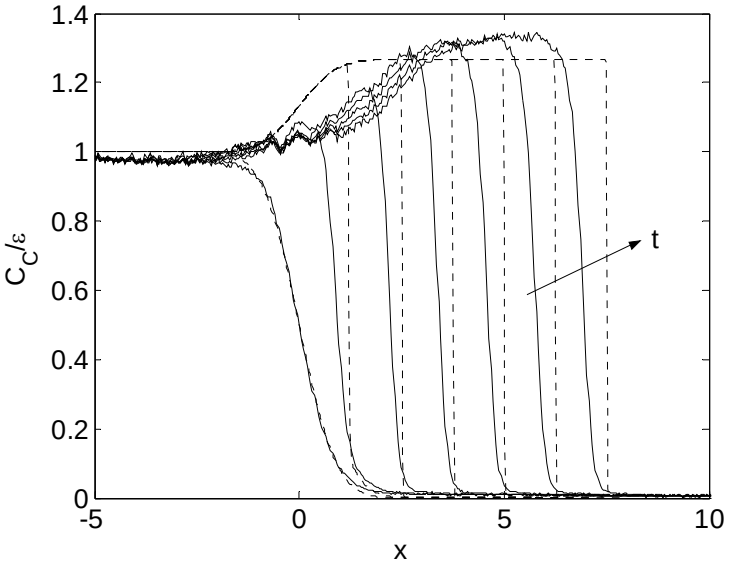

Figure 4: Comparison of measured and predicted sample ion concentration profiles for $\gamma = 5$, $\varepsilon = 1$ and $\beta = 0.25$. Model predictions are shown as dotted lines. The time between each curve is 33 ms. The sample was bodipy dye and the co-ion was the chloride ion.

For quantitative analysis of the CCD images, a background image is subtracted from the raw image and this difference is normalized by the difference between a flatfield and the background image.[12] To compare the two dimensional image data with the one-dimensional model, the intensity data for the pixel regions of the microchannel images were averaged along the vertical direction (along the width of the channels, as indicated in Figure 3b) to form one dimensional axial intensity profiles. Figures 4 shows the temporal development of the sample ion concentration distribution for $\gamma = 5$. The sample ion concentration increases to a maximum value of 1.3 which is much lower than γ. Once this concentration enhancement is achieved, the axial width of the stacked region continues to grow without further increase in peak concentration value, as predicted by the model. Figure 4 also shows an overlay comparison between model predictions and experimentally measured concentration profiles. There is good qualitative comparison in terms of the peak shapes and the temporal growth of the maximum concentration. The model neglects diffusion and convective effects, whereas in the experiments these effects lead to a slight broadening of sample profiles. The simple electromigrational model therefore over predicts the rate at which concentration enhancement occurs. In contrast, the absolute value of maximum concentration enhancement in not a function of diffusive and convective dispersion fluxes and is therefore in very good agreement with the experiments as shown in Figure 5. The error bars represent 95% confidence interval over five realizations for the three cases. These detailed comparison of the predicted and measured dynamics show that the electromigrational model can be used to quantitatively predict maximum concentration enhancement and approximately predict the rate of enhancement and the shape of concentration profiles. The model should be useful in optimizing FASS experiments with finite ε values.

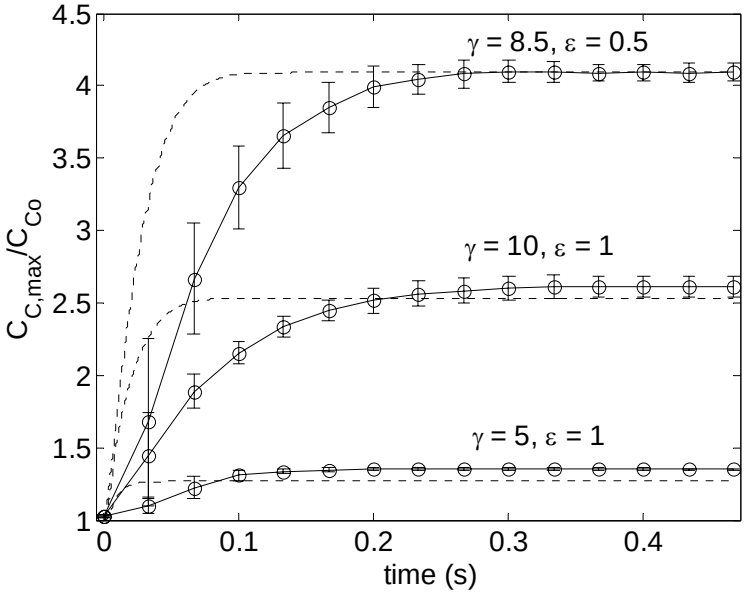

Figure 5: Normalized sample ion peak concentration versus dimensional time for three values of γ and two values of ε. The dotted lines are the model predictions and the circles are experimental results. The model under predicts the rate of concentration increase but well predicts the absolute value of concentration enhancement.

CONCLUSIONS

We have developed an electromigration model to investigate the coupled, nonlinear dynamics of three fully ionized species across single electrolyte-electrolyte interface. We solved the resulting nonlinear hyperbolic equation using finite volume methods and conducted a parametric study. Strength of the sample overloading effects is determined by ε, the ratio of the initial sample concentration to that of the initial counter-ion concentration in the sample region. For negligible values of ε, the maximum concentration enhancement approaches the ideal limit equal to γ. For finite values of ε, model predictions shows that there are two distinct regimes of concentration enhancement. Transition between the two regimes is governed by β, the dimensionless ratio of the product of electrophoretic mobility and valence number of the sample ion and the co-ion. The regimes are as follows:

- For $\beta > 1$, the sample ion concentration field in the single electrolyte-electrolyte case is characterized by a rarefaction wave and maximum concentration enhancement is greater than γ.
- For $\beta < 1$, the sample ion concentration wave in the single electrolyte-electrolyte case develops sharp gradients and tends toward an concentration shock wave. For $\beta < 1$ cases, the maximum concentration enhancement is always less than γ.

We have experimentally validated the model for the $\beta < 1$ regime by using scalar epi-fluorescence imaging to measure the sample ion concentration fields. There is good qualitative comparison between the model predictions of the sample ion concentration profiles. There is good quantitative comparison between the absolute values of predicted and measured maximum concentration enhancement. Improved understanding of FASS process would be further aided by development of multi-species, electromigration-diffusion-convection models, which include equilibrium reactions and which can handle the finite ε regime. Such tools would help to optimize ultra-high concentration FASS systems involving very low conductivity buffers or DI water as the sample matrix.

ACKNOWLEDGEMENT

This work was sponsored by DARPA (Contract Number F30602-00-2-0609) with Dr. Anantha Krishnan as contract monitor and by an NSF CAREER Award (J.G.S.) with Dr. Michael W. Plesniak as contract monitor.

REFERENCES

(1) Burgi, D. S., Chien, R. L. *Anal. Chem.* **1991**, *63*, 2042-2047.
(2) Chien, R. L., Burgi, D.S. *J. Chromatogr.* **1991**, *559*, 141-152.
(3) Chien, R. L., Burgi, D.S. *Anal. Chem.* **1992**, *64*, 1046-1050.
(4) Jung, B., Bharadwaj, R., Santiago, J. G. *Electrophoresis* **2003**, *24*, 3476-3483.
(5) Lichtenberg, J., Verpoorte, E., Rooij, N. F. *Electrophoresis* **2001**, *22*, 258-271.
(6) Yang, H., Chien, R. L. *J. Chromatogr. A* **2001**, *924*, 155-163.
(7) Kuban, P., Berg, M., Garcia, C., Karlberg, B. *J. Chromatogr. A* **2001**, *912*, 163-170.
(8) Bharadwaj, R., Santiago, J. G. *Anal. Chem.* **2004 (Submitted)**.
(9) Chien, R. L. *Anal. Chem.* **1991**, *63*, 2866-2869.
(10) Bharadwaj, R., Santiago, J. G. *Anal. Chem.* **2004 (Submitted)**.
(11) Foret F., K., L., Bocek, P. *Capillary Zone Electrophoresis*; VCH publishers Inc.: New York, 1993.
(12) Bharadwaj, R., Santiago, J. G., Mohammadi, B. *Electrophoresis* **2002**, *23*, 2729-2744.
(13) Preisler, J., Yeung, E. S. *Anal. Chem.* **1996**, *68*, 2885-2889.